Identification of Peptide Antagonists to Glycoprotein Ibα That Selectively Inhibit von Willebrand Factor Dependent Platelet Aggregation

Susan Adam Benard,[‡,§] Thomas M. Smith,[‡,||,⊥] Kristina Cunningham,[§] Jaison Jacob,[||] Thamara DeSilva,[§] Laura Lin,[§] Gray D. Shaw,[||] Ron Kriz,[§] and Kerry S. Kelleher*[,§]

Departments of Chemical and Screening Sciences and Cardiovascular and Metabolic Disease, Wyeth Research, 200 CambridgePark Drive, Cambridge, Massachusetts 02140

Received December 12, 2007; Revised Manuscript Received February 4, 2008

ABSTRACT: GPIbα is an integral membrane protein of the GPIb-IX-V complex found on the platelet surface that interacts with the A1 domain of von Willebrand factor (vWF-A1). The interaction of GPIbα with vWF-A1 under conditions of high shear stress is the first step in platelet-driven thrombus formation. Phage display was used to identify peptide antagonists of the GPIbα−vWF-A1 interaction. Two nine amino acid cysteine-constrained phage display libraries were screened against GPIbα revealing peptides that formed a consensus sequence. A peptide with sequence most representative of the consensus, designated PS-4, was used as the basis for an optimized library. The optimized selection identified additional GPIbα binding peptides with sequences nearly identical to the parent peptide. Surface plasmon resonance of the PS-4 parent and two optimized synthetic peptides, OS-1 and OS-2, determined their equilibrium dissociation GPIbα binding constants (K_Ds) of 64, 0.74, and 31 nM, respectively. Isothermal calorimetry corroborated the K_D of peptide PS-4 with a resulting affinity value of 68 nM. An ELISA demonstrated that peptides PS-4, OS-1, and OS-2 competitively inhibited the interaction between the vWF-A1 domain and GPIbα-Fc in a concentration-dependent manner. All three peptides inhibited GPIbα−vWF-mediated platelet aggregation induced under high shear conditions using the platelet function analyzer (PFA-100) with full blockade observed at 150 nM for OS-1. In addition, OS-1 blocked ristocetin-induced platelet agglutination of human platelets in plasma with no influence on platelet aggregation induced by several agonists of alternative platelet aggregation pathways, demonstrating that this peptide specifically disrupted the GPIbα−vWF-A1 interaction.

Glycoprotein Ib-IX-V is a protein receptor complex found in the platelet plasma membrane that initiates the rolling and arrest of platelets at sites of vascular injury (reviewed in refs *1*−*3*). These events are initiated by the actions of von Willebrand factor (vWF)[1] bound to exposed collagen in the subendothelial matrix. Under conditions of high or turbulent hydrodynamic shear stress, vWF is thought to undergo a conformational change exposing a normally cryptic binding site for the GPIb-IX-V complex within its A1 domain (*4, 5*). The binding of the GPIb-IX-V complex to vWF initiates a cascade of events including platelet attachment, platelet shape change and spreading along the exposed subendothelium, release of granule contents, and ultimately platelet recruitment and aggregation via activation of the platelet GPIIb/IIIa receptor in a Src family kinase dependent mechanism (*6*–*8*).

The GPIb-IX-V receptor complex is comprised of four transmembrane polypeptides, GPIbα, GPIb*β*, GPIX, and GPV (reviewed in ref *2*). The only protein of the GPIb-IX-V complex demonstrated to interact with vWF is GPIbα. The crystal structures of GPIbα and the GPIbα binding domain of vWF (vWF-A1) (*9, 10*) determined that the extracellular amino-terminal 290 amino acids of GPIbα interact with the A1 domain of vWF (*11, 12*). The GPIbα and vWF-A1 domain complex structure reveals two distinct regions of protein interaction. One contact site on GPIbα is located near the amino terminus consisting of a *β*-hairpin turn (*β*-finger). The second, a larger and more extensive region of GPIbα (*β*-switch), undergoes a conformational change to a *β*-hairpin structure after complex formation (*13, 14*). The conformational status of the *β*-switch of GPIbα is a critical factor affecting the affinity of these two proteins for one another.

Disrupting one of these two distinct GPIbα-vWF interaction sites may present a powerful strategy for reducing platelet-driven thrombus formation and provide an attractive

* To whom correspondence should be addressed. Tel: 617-665-5093. Fax: 617-665-5419. E-mail: KKelleher@Wyeth.com.

‡ These authors contributed equally to this work.

§ Department of Chemical and Screening Sciences, Wyeth Research.

|| Department of Cardiovascular and Metabolic Disease.

⊥ Current address: Novartis Institutes for Biomedical Research, Lead Finding Platform, 250 Massachusetts Ave., Cambridge, MA 02139.

[1] Abbreviations: GPIbα, glycoprotein Ib α; vWF, von Willebrand factor; MEM, modified Eagle's media; SDS, sodium dodecyl sulfate; HRP, horseradish peroxidase; PCR, polymerase chain reaction; PRP, platelet-rich plasma; PPP, platelet-poor plasma; SPR, surface plasmon resonance; HP, high performance; ELISA, enzyme-linked immunosorbent assay; NMR, nuclear magnetic resonance; PFA, platelet function analysis; HTS, high-throughput screen; PAGE, polyacrylamide gel electrophoresis; TBS, Tris-buffered saline; PBS, phosphate-buffered saline; CHO, Chinese hamster ovary; K_D, equilibrium dissociation constant; TU, transforming unit; mAb, monoclonal antibody; DMSO, dimethyl sulfoxide; PNPP, *p*-nitrophenyl phosphate disodium salt; HPLC, high-performance liquid chromatography; SA, streptavidin; ITC, isothermal titration calorimetry; ADP, adenosine diphosphate; RU, resonance units; VWD, von Willebrand disease; IC_{50}, half-maximal inhibitory concentration.

10.1021/bi702428q CCC: $40.75
Published on Web 03/26/2008

target for drug discovery. Unfortunately, significant challenges exist in identifying small-molecule inhibitors of protein–protein interactions (*15*). Typically proteins interact across multiple interfaces that involve large flat surfaces without well-defined pockets. Previous work demonstrated that high-affinity ligands for protein targets could be selected from peptide libraries displayed on bacteriophage (*16*), and more recent investigations have identified peptides capable of disrupting protein contacts by binding to a single preferred protein–protein interaction surface or "hot spot". Hot spots occupy a small portion of the protein interface and are the energetic focus of the protein–protein interaction (*17*). They are frequently hydrophobic in nature, accessible, and have a high degree of plasticity. Considering that peptides have been shown to preferentially bind at hot spots, targeting this region with a peptide inhibitor may provide a useful reagent to assist small-molecule drug discovery (*18, 19*).

Phage display was used to achieve this goal of identifying a peptide inhibitor and support traditional high-throughput screening efforts to identify a small-molecule drug lead (*15*). Multivalent phage display has the benefit of cooperative binding and as a result can identify peptide hits with a wide range of affinities. Optimizing the peptide sequence further refines those peptide–protein interactions most critical for binding. The synthetic counterparts of the phage display peptides, once demonstrated to bind the target protein and compete with the natural ligand, validate HTS efforts to obtain small-molecule antagonists of a protein–protein interaction. These peptide antagonists indicate the potential presence of a drug-like site on the target protein. In addition, peptides are easily obtainable reagents for assay development and a subsequent HTS (*20*).

X-ray costructures of peptides and HTS lead compounds with the target protein can generate complementary information useful for rational drug design efforts (*21, 22*). Peptide costructures aid in the identification of functional groups presented by peptide side chains and have provided helpful insights into the design of small molecules used to inhibit platelet aggregation by interaction with glycoprotein IIb/IIIa (*21*). In addition, these costructures can identify amino acids from the target essential to the peptide–protein interaction. In general, peptide and compound costructures can supply insights into the chemistry of protein binding sites and their interaction motifs (*23*) and guide medicinal chemistry efforts for the rational design of a small-molecule drug (*24, 25*).

Here we report the use of phage display to identify novel disulfide-constrained peptides capable of blocking the interaction between GPIbα and vWF-A1. Ultimately, these peptides will be used for obtaining costructure information to support the development of small-molecule GPIbα antagonists.

EXPERIMENTAL PROCEDURES

Generation of Recombinant GPIbα Constructs. The polymerase chain reaction was used with a full-length wild-type GPIbα cDNA to amplify the coding sequence of the first 290 amino acids of human GPIbα. The PCR fragment was restriction enzyme digested with *Xba*I and *Not*I and ligated into the mammalian expression vector pED containing the coding sequence for the human IgG1 Fc domain (designated GPIbα-Fc). An enterokinase cleavage site was incorporated between GPIbα and the Fc domain. The DNA sequence of the construct (GPIbα-Fc pED) was confirmed using an Applied Biosystems 3730 automated capillary sequencer following the manufacturer's recommendations (Applied Biosystems Inc., Foster City, CA).

Expression and Purification of Recombinant GPIbα Proteins. GPIbα-Fc pED was transfected into CHO-DUKX cells using lipofectin (Gibco BRL) and grown in MEM α media supplemented with 10% fetal bovine serum, 200 units/mL each penicillin and streptomycin, 2 mM L-glutamine, and 200 nM methotrexate (Sigma). R1CD1 (JRH Biosciences) media containing 2 mM L-glutamine and 200 units/mL each penicillin and streptomycin were added to semiconfluent cell cultures, and the conditioned medium was harvested and replaced every 24 h for 3 days. The filtered conditioned medium was concentrated using an Amicon RA2000 ultrafiltration system with a membrane cutoff of 10000 Da. The medium was adjusted to 25 mM Tris-HCl, pH 8, and 150 mM NaCl and loaded onto a protein A−Sepharose column (Amersham Biosciences). The column was washed in Tris-buffered saline (TBS) and eluted with Immunopure IgG elution buffer (Pierce). Adding $^1/_{10}$th volume of 1 M Tris-HCl, pH 8, immediately neutralized protein fractions. The fractions were concentrated (Amicon Microcon YM-10) and dialyzed against phosphate-buffered saline (PBS). Protein concentration was determined by A_{280} measurements using the extinction coefficient. The protein was evaluated by SDS−PAGE using 4–12% Bis-Tris gels (Invitrogen) and Coomassie blue staining and determined to be more than 95% pure. The recombinant GPIbα-Fc fusion protein was used for the competitive ELISA and isothermal titration calorimetry studies. Monomeric GPIbα protein minus the Fc fusion protein (residues 1–290, designated GPIbα monomer) was used for all phage display panning, NMR, and SPR binding studies and was produced by digestion of the dimeric GPIbα-Fc with enterokinase. The liberated GPIbα-monomer protein was further purified by gel filtration chromatography on a HiTrap Q-Sepharose HP column (Amersham Biosciences). The production of the A1 domain of vWF has been described previously (*14*).

GPIbα Phage Display Selection. A phage display selection was performed against the GPIbα monomer using two cysteine-constrained 9 amino acid random peptide libraries, CX_9C and $CX_9W_{1-9}C$. The $CX_9W_{1-9}C$ library was designed to contain at least one tryptophan residue in every phage-displayed peptide. The CX_9C library contained an estimated 7.0×10^8 independent peptide sequences. Both libraries were constructed using the M13 filamentous bacteriophage peptide display cloning system from New England Biolabs (NEB, Beverly, MA). Expressing the peptide as a fusion with the M13 minor coat protein gene III presents as many as five copies of the peptide clustered on the surface of the bacteriophage. GPIbα monomer was used as the target protein instead of GPIbα-Fc to avoid the selection of Fc binding peptides. The GPIbα monomer was biotinylated (GPIbα-biotin) using sulfo-NHS-LC biotin from Pierce (Rockford, IL) following the manufacturer's protocol. In all three rounds of selection, two neutravidin-coated microplates (Pierce) were blocked with SuperBlock (Pierce) and washed with TBST (Tris-buffered saline, 50 mM Tris-HCl, pH 7.4, 150 mM NaCl, and 0.1% Tween 20). Phage that bind to plastic and SuperBlock were subtracted by adding 2×10^{11}

Table 1: Primary Selection (PS) Phage Peptide Sequences

Position	0	1	2	3	4	5	6	7	8	9	10
PS-1	C	S	E	R	Q	A	L	H	G	W	C
[a]PS-2	C	D	E	K	R	A	L	H	N	L	C
[b]*PS-3	C	N	E	R	A	A	L	W	N	L	C
*PS-4	C	T	E	R	W	A	L	H	N	L	C
*PS-5	C	E	S	R	W	W	L	R	N	A	C
PS consensus	**C**	**X**	**E/S**	**R/K**	**X**[c]	**A/W**	**L**	**X**	**N/G**	**X**	**C**

[a] Identical residues are shaded in gray, and those outlined have similar polarity or hydrophobicity. [b] Peptides marked with an asterisk were isolated from the W-enriched library. [c] The greatest amino acid diversity is at position 4.

phage transducing units (TU) to one of the microplates and incubating for 1 h at 4 °C. GPIbα-biotin was added to the second microplate at a concentration of 2 μg/mL and captured by neutravidin for 1 h at room temperature. The subtracted phage were transferred to the GPIbα-biotin-coated plate and incubated for 4 h at room temperature. Following incubation, 2 μL of 10 mM biotin was added to eliminate neutravidin-binding phage. A nonspecific acid elution with 0.2 M glycine, pH 2.2, was performed and neutralized with 1 M Tris-HCl, pH 9.1.

Optimized Phage Display Selection. The primary selection peptide PS-4 was used as the basis for constructing an optimized library (Table 1). This library was designed to retain the amino acids of the primary selection peptide at a frequency of 25−50% and had an estimated molecular diversity of 1.4×10^6 independent peptide sequences (*26, 27*). This CX_9C optimized library was constructed as previously described and screened against GPIbα-biotin. The optimized selection was identical to the primary selection with the exception of a specific elution with 20 μM PS-4 for 45 min at room temperature. In addition, to eliminate phage binding to SuperBlock, the blocking reagent in the final round of selection was changed to BSA (Pierce).

Phage Peptide Analysis by ELISA. An ELISA was used to identify phage-displayed peptides that bind to GPIbα monomer. A neutravidin-coated microplate was incubated with SuperBlock for 30 min at 4 °C followed by capture of 1 μg/mL GPIbα-biotin for 1 h at 4 °C. A control plate was also incubated with SuperBlock, and 1×10^8 TUs of phage were added to each microplate and allowed to bind for approximately 2 h at 4 °C. GPIbα-biotin binding phage were detected with a horseradish peroxidase (HRP) conjugated anti-M13 mAb from Amersham Biosciences (Piscataway, NJ) and standard substrate reagents. ELISA positive clones were sequenced as previously described.

Competitive ELISA of GPIbα-Fc Binding to vWF-A1 Protein and Inhibition by Peptides. An ELISA was utilized to assess GPIbα-Fc binding to vWF-A1 and to examine peptide inhibition of this interaction. The vWF-A1 protein was diluted to 20 μg/mL in TBS, pH 7.5, and 100 μL was added to a microplate and allowed to bind at 4 °C overnight. The wells were blocked with 1% BSA (w/v) diluted in TBS, incubated at room temperature for 2 h, and washed with TBS, pH 7.5, and 0.05% Tween-20. A 100 μL volume of 20 μg/mL GPIbα-Fc in protein dilution buffer (TBS, pH 7.5, 0.05% Tween-20, 0.2% BSA) was added to each well, along with a 1.25% DMSO control vehicle or the appropriate concentration of peptide in DMSO, and mixed for 1.5 h. After washing, goat anti-human IgG alkaline phosphatase (Southern Biotech) was added to the wells and incubated for 1 h. Color was developed with alkaline phosphatase diethanolamine substrate buffer (Pierce) prepared with 5 mg of PNPP per 5 mL. The enzymatic reaction was stopped by the addition of 50 μL of 2 N NaOH and the absorbance read at 405 nm.

Binding Affinity Analysis Using BIAcore. Surface plasmon resonance with a BIAcore 3000 biosensor system (BIAcore, Uppsala, Sweden) was used to determine the equilibrium dissociation constant (K_D) between GPIbα monomer and several peptides (AnaSpec, San Jose, CA). Synthetic phage peptides were appended with residues from M13 gene III, alanine at the amino terminus and two glycines at the carboxy terminus as those residues encoded by gene III may impact binding. The peptides were >95% pure as determined by mass spectroscopy (MS) and HPLC analyses. Approximately 1000 RUs of GPIbα-biotin was immobilized on a streptavidin-coated sensor chip (SA) by noncovalent capture according to the manufacturer's protocols. A titration series was performed with each peptide analyte, and the BIAevaluation 3.0 kinetic or equilibrium model was used to determine the K_D.

Isothermal Titration Calorimetry. The interaction of peptide PS-4 with GPIbα-Fc was determined using an isothermal titration calorimeter, VP-ITC (MicroCal Inc., Northampton, MA). The peptide and protein solution buffer was 50 mM Tris-HCl (pH 7.5) and 100 mM NaCl. Experiments were performed at a working volume of 1.41 mL, 25 °C, and a stir rate of 310 rpm. Titration of the 102 μM peptide was performed with a single 2 μL injection followed by 34 8 μL injections into 4 μM GPIbα-Fc with 300 s between injections. Three separate experiments yielded similar results. Heats of dilution were subtracted from the corresponding heats of reaction to obtain the heat due solely to peptide binding to protein. Analysis of the data was performed using Origin 7.0 (MicroCal), the model for a single class of binding sites.

NMR Binding Analysis of Peptides and Competition with vWF-A1. NMR experiments were performed on a Bruker Avance II spectrometer operating at 700.14 MHz. All experiments were carried out at 25 °C in a buffer containing 50 mM Tris-d_{11} and 250 mM NaCl in 90:10 H_2O:D_2O. ^1H NMR spectra were obtained using the 3-9-19 sequence for water suppression. The 8K complex points were collected with an interscan delay of 2 s for 512 scans. The data were apodized using a cosine-squared bell and zero filled before Fourier transformation.

PFA-100 Analysis and Inhibition by Peptides. A PFA-100 assay was performed with human blood collected into vacutainer tubes, containing 3.2% sodium citrate as the anticoagulant, from volunteers who had not taken any platelet inhibitory medications over the previous 2 weeks. A 5 μL aliquot of peptide dissolved in 25% DMSO was added to 1 mL of whole human blood to give the respective peptide concentration and a final DMSO concentration of 0.125%. Tubes were inverted 10 times to mix and allowed to sit at room temperature for 5 min prior to analysis with the PFA-100 instrument. Collagen/epinephrine cartridges (Dade Behring) were used for the PFA-100 assay following the manufacturer's protocol. Closure times of 80 ± 4 s were obtained with 0.125% DMSO alone in whole blood.

In Vitro Platelet Aggregation Assay in an Optical Aggregometer. A platelet aggregation assay was performed with human blood collected, as described above, from volunteers. Platelet-rich plasma (PRP) was generated by centrifugation in a Sorvall Legend RT centrifuge with a swinging bucket rotor at 450*g* for 10 min. The cloudy yellow supernatant was removed, and the remaining blood was centrifuged at 2000*g* for 10 min to generate platelet-poor plasma (PPP). Platelets were counted and diluted to 2.5×10^8 platelets/mL with PPP. The assay was set up in a Chronolog aggregometer, model 560CA (Chronolog Corp.), cuvette as follows: 245 μL of PRP, 2.5 μL of peptide in 25% DMSO, and a control using 25% DMSO alone. After mixing, the solution was incubated at 37 °C for 5 min. A stable baseline recording was made for 1 min, then 2.5 μL of each agonist was added to the final concentrations indicated (ristocetin, 1 mg/mL; ADP, 20 μM; collagen, 10 μg/mL; and γ-thrombin, 4 μg/mL), and the tracing was allowed to record for an additional 4 min. Peptides were dissolved in 25% DMSO and diluted 50-fold into the PRP prior to the initiation of aggregation with agonist.

RESULTS

Phage Display Primary GPIbα Selection. Two cysteine-cyclized 9 amino acid phage peptide libraries, CX_9C and $CX_9W_{1-9}C$, were constructed to screen and identify antagonists of GPIbα. Purified GPIbα monomer was biotinylated and captured on neutravidin-coated microplates. After completing three rounds of selection, 480 individual phage clones were evaluated by ELISA to identify those that bind specifically to GPIbα-biotin. Sequencing the immunopositive clones revealed an emerging consensus (Table 1) that was not found within the vWF-A1 protein sequence.

The sequences of the GPIbα-selected phage peptides were remarkably similar with the exception of the diversity observed at amino acid position 4 (Table 1). Both peptides PS-4 and PS-5 contain hydrophobic tryptophan residues at position 4 and were isolates of the $CX_9W_{1-9}C$ library that was designed to possess at least one tryptophan for each phage-displayed peptide. Phage peptide PS-3, also from library $CX_9W_{1-9}C$, had conserved residues at all positions with the exception of a hydrophobic alanine (A) at position 4. PS-1 and PS-2 contained a polar glutamine (Q) or charged arginine (R) residue at position 4, and amino acids at the remaining positions were almost entirely conserved. PS-4 was chosen as the basis of an optimized library because its sequence was most representative of the primary selection consensus.

Phage Display Optimized GPIbα Selection. The optimization of PS-4 was undertaken to improve its binding and inhibitory properties. An optimized nine amino acid library, CX_9C, was designed with fixed cysteines, and amino acids from the parent peptide sequence were retained at a theoretical frequency between 25% and 50%. The theoretical amino acid frequency is determined from the nucleotide sequence by comparing the number of codons for a given amino acid in the synthetic library primer to the total number of codons for each amino acid. The optimized library contained an estimated 1.4×10^6 independent peptide sequences, as determined by population sampling, and was screened against the target protein GPIbα monomer in a manner similar to the primary selection.

Table 2: Optimized Selection (OS) Peptide Sequences

PS-4	C	T	E	R	W	A	L	H	N	L	C
Position	0	1	2	3	4	5	6	7	8	9	10
0S-1	C	T	E	R	M	A	L	H	N	L	C
0S-2	C	T	E	R	D	A	L	H	N	L	C
0S-3	C	T	E	R	L	A	L	H	N	L	C
0S-4	C	S	E	R	W	A	L	H	N	L	C
0S-5	C	S	E	R	A	A	L	H	N	L	C
0S-6	C	S	E	R	M	A	L	H	N	L	C
Optimized consensus	[a]C	S/T	E	R	[b]X	A	L	H	N	L	C

[a] The peptide sequences from the optimized library refined the consensus sequence. Residues shaded in gray are identical, and those outlined have similar polarity. [b] The residues at position 4 exhibit a greater degree of diversity than seen at the other positions.

An ELISA was performed on 144 clones from the optimized selection, and 36 candidates bound specifically to GPIbα. Representative sequences are shown in Table 2. Sequence analysis revealed the amino acids from the parent peptide were almost entirely retained with the exception of the residues at position 4 where again diversity was observed similar to the results of the primary selection. Analysis of these peptide sequences revealed that the tryptophan (W) at position 4 was most often replaced by methionine (M), aspartate (D), or leucine (L). The observed frequencies of M, D, and L were 30%, 8.7%, and 35% versus the expected values of 0.5%, 0.5%, and 4.5%, respectively. The ratios of observed to expected frequencies suggested a stronger selective preference for M and D residues. As a result of the disparity between expected and observed amino acid frequencies, and the potential for an improvement in binding affinity, peptides with an M or D at position 4 were chosen for synthesis and further analysis.

Surface Plasmon Resonance of Phage Display Peptides with BIAcore. SPR analysis of synthetic peptides from the primary and optimized selections was undertaken to determine the K_D values between each peptide and GPIbα-biotin monomer (Figure 1). The synthetic primary selection peptide PS-4 and two optimized selection peptides OS-1 and OS-2 were appended with three adjacent M13 gene III residues due to their potential to impact binding affinity. Approximately 1000 RUs of GPIbα-biotin was immobilized on a streptavidin-coated chip using the manufacturer's protocol. The primary selection peptide PS-4 had a K_D of 64 nM and optimized selection peptides OS-1 and OS-2 had K_D values of 0.74 and 31 nM, respectively. Only the optimized peptide OS-1 showed significant improvement in binding affinity compared to PS-4. Peptide OS-1 with an M for W substitution at position 4 resulted in nearly a 90-fold improvement in K_D whereas the change to D within peptide OS-2 had a minimal effect (Table 3).

Isothermal Titration Calorimetry. The interaction of peptide PS-4 with GPIbα-Fc was also studied by isothermal titration calorimetry (ITC) to obtain binding affinity, stoichiometry, and thermodynamic data. Figure 2 shows a representative calorimetric trace (Figure 2A) and the corresponding titration curve (Figure 2B) obtained at 25 °C by titration of GPIbα-Fc (4 μM) with 8 μL aliquots of peptide PS-4 (102 μM). The integrated heats represent the net heats

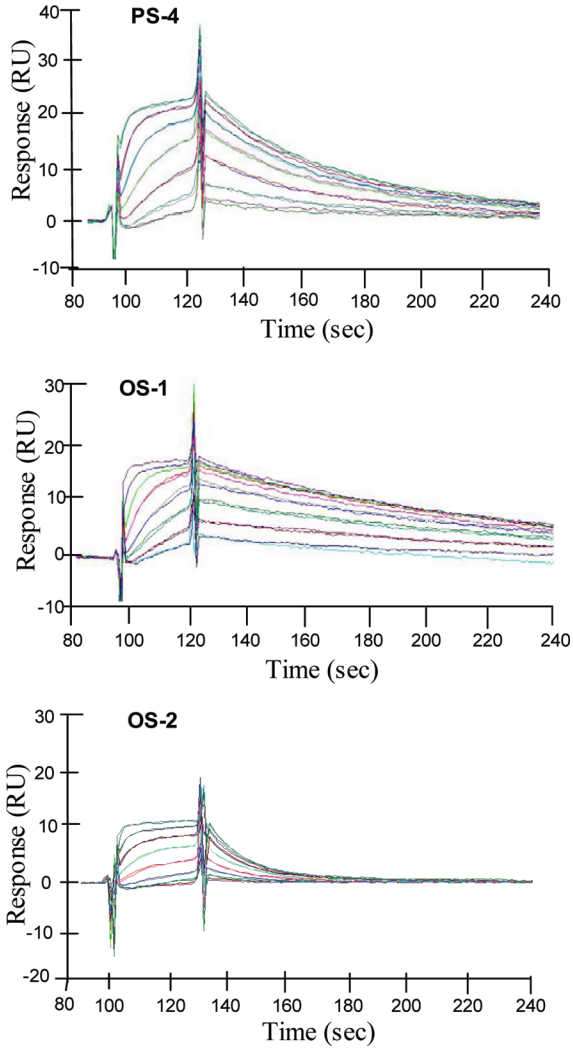

FIGURE 1: SPR analysis of synthetic peptides. Surface plasmon resonance was used to determine the affinity between GPIbα monomer and PS-4, OS-1, and OS-2. Approximately 1000 RUs of GPIbα-biotin were immobilized on a streptavidin-coated sensor chip. A titration series was performed with each peptide analyte (PS-4, 7.8−1000 nM; OS-1, 0.78−100 nM; and OS-2, 3.9−500 nM), and kinetic or equilibrium analysis was used to fit the sensogram traces and determine the K_D values for PS-4, OS-1, and OS-2 (64, 0.74, and 31 nM, respectively).

of each injection after subtracting the dilution heats of PS-4 into buffer. The downward direction of the titration peaks and the corresponding negative integration heats indicate that binding of PS-4 to GPIbα-Fc is an exothermic reaction. ITC data fit well to a model for a single class of binding sites resulting in an affinity value of 68 nM, a stoichiometry of 1.04 PS-4 peptide per GPIbα-Fc, and an enthalpy of binding (ΔH) of −12 kcal/mol. The 68 nM affinity measurement of PS-4 peptide to GPIbα-Fc obtained by ITC corroborates the 64 nM value obtained by SPR analysis for the GPIbα monomer and suggests that the enterokinase flanking sequence and Fc domain did not influence the binding affinity. In addition, the stoichiometry of the binding interaction supports site-specific independent binding of PS-4 to each GPIbα-Fc monomer.

NMR Binding Studies of OS-1 and Competition with vWF-A1. The submicromolar binding affinity of peptide OS-1 to GPIbα-Fc allowed the NMR evaluation of peptide binding on the interaction between vWF-A1 and GPIbα-Fc. Fortunately, unbound vWF-A1 has a well-resolved signal at ca. 5.9 ppm in the ^{1}H NMR spectrum as seen in Figure 3. The response of this signal was monitored as GPIbα-Fc was titrated into 20 μM vWF-A1. The addition of GPIbα-Fc to a final concentration of 5 μM results in line broadening indicating that vWF-A1 and GPIbα-Fc form a complex and that vWF-A1 is exchanging between bound and free forms. Further addition of GPIbα-Fc to 10 μM causes complete obliteration of this peak even at this substoichiometric ratio. However, the addition of OS-1 to 20 μM partially reverses line broadening as is evidenced by spectrum D in Figure 3, implying that OS-1 and vWF-A1 share a common GPIbα-Fc binding site.

Competitive ELISA of GPIbα Binding Peptides. A competitive ELISA was performed to determine the ability of PS-4, OS-1, and OS-2 to inhibit the vWF-A1 and GPIbα interaction. The binding between vWF-A1 and GPIbα-Fc was measured in the presence of increasing concentrations of peptide (Figure 4A). OS-1 had a calculated IC_{50} value of 510 nM, a more than 2-fold improvement compared to the IC_{50} values determined for PS-4 and OS-2, 1260 and 1400 nM, respectively (Table 3).

PFA-100 under High Shear To Evaluate the Inhibitory Properties of Peptides. The inhibition of platelet aggregation with synthetic peptides PS-4, OS-1, and OS-2 was measured using flow cytometry and the platelet function analyzer (PFA-100) under high shear stress to simulate the conditions of physiological hemostasis. PFA-100 collagen/epinephrine cartridges were used to perform the initial screen for platelet aggregation. At the concentration of 1 μM, PS-4, OS-1, and OS-2 were able to block high shear-induced platelet aggregation as shown by a closure time of 300 s (Figure 4B). A dilution series of each peptide revealed that OS-1 was approximately 8-fold more potent than the parent peptide PS-4, as a maximal closure time of 300 s was still evident at an OS-1 concentration of 150 nM (Table 3). This significant increase in closure time observed only after adding the peptide inhibitors indicated that the collected donor platelet samples were normal and free of acetylsalicylic acid, negating the need for subsequent testing with collagen/ADP cartridges.

Effect of GPIbα Binding Peptide on Platelet Aggregation Induced by Multiple Agonists. A platelet optical aggregation assay was performed with peptide OS-1, due to its strong binding affinity, to evaluate inhibition specificity for the GPIbα pathway. The assays were performed in the presence of three agonists not acting directly through the GPIbα pathway and ristocetin, an agonist specific for GPIbα signaling. Collagen, ADP, and thrombin induced a robust aggregation response in vehicle-treated human platelets as shown in Figure 5. The addition of 20 μM OS-1 to these reactions did not alter the rate of aggregation. However, inhibition was observed when 20 μM OS-1 was added to the ristocetin-treated platelets, indicating that this peptide is specifically targeting the GPIbα pathway. Complete inhibition of ristocetin-induced platelet aggregation was observed using concentrations of OS-1 peptide as low as 31 nM.

DISCUSSION

Disrupting the interaction between GPIbα and vWF to modulate platelet adhesion, activation, and thrombosis

Table 3: Characterization of Synthetic Peptides

Position 1 2 3 4 5 6 7 8 9	Binding	[b]Competition	
	K_D nM	IC50 nM	PFA100 nM
PS-4 **Ac-A C T E R W A L H N L C G G-NH_2**	64	1260	1250
OS-1 Ac-A C T E R **M** A L H N L C G G-NH_2[a]	0.74	510	150
OS-2 Ac-A C T E R **D** A L H N L C G G-NH_2	31	1400	1250

[a] The underlined M or D residues were substituted for the W at position 4 in the optimized selection. The W to M substitution resulted in nearly a 90-fold improvement in binding affinity determined by SPR, where the change to D improved the K_D only 2-fold. [b] IC_{50} values were determined using a competitive ELISA and PFA-100 assay.

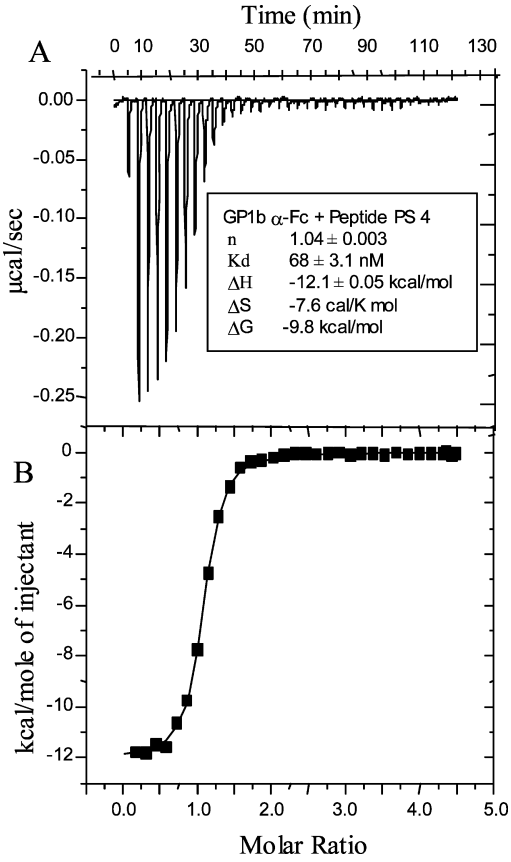

FIGURE 2: Titration of peptide PS-4 into GPIbα-Fc. (A) Calorimetric trace obtained at 25 °C by titration of PS-4 into a solution of GPIbα-Fc. Each peak corresponds to an 8 μL injection (at 300 s intervals) of PS-4 into the calorimetric cell, except for the first peak that results from a 2 μL injection. (B) Heats of reaction (integrated from the calorimetric trace) plotted as a function of the PS-4/GPIbα-Fc molar ratio. The solid line is the best fit to the experimental data (■), and thermodynamic parameters appear in the inset.

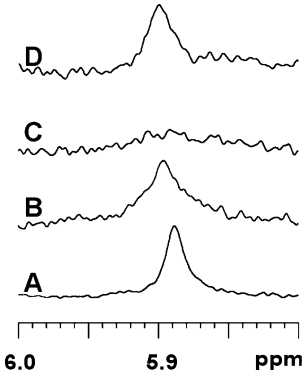

FIGURE 3: NMR binding studies of optimized peptide OS-1. vWF-A1 at a concentration of 20 μM has a well-resolved 5.9 ppm signal (A). This signal undergoes exchange broadening upon addition of 5 μM GPIbα (B). Even at a substoichiometric concentration of 10 μM GPIbα, the signal from vWF-A1 is completely obliterated (C). When 20 μM OS-1 is added to this complex, the signal recovers partially, suggesting competition (D).

presents a significant challenge for drug discovery. Investigators have previously reported a variety of antibody, protein, and peptide antagonists of this interaction that target either GPIbα or vWF. Antagonists to vWF include the humanized anti-vWF monoclonal antibody, AJW200, reported to inhibit ristocetin-induced platelet aggregation upon intravenous administration to monkeys (*28*). A second vWF antagonist, GPG-290, containing the 290 amino-terminal residues of GPIbα, was validated as a GPIbα-vWF inhibitor using a canine deep vessel wall injury model (*29, 30*). Lastly, the in vivo administration to nonhuman primates of a recombinant 225 amino acid disulfide constrained peptide fragment corresponding to amino acids 504−728 of the human vWF binding domain was demonstrated to reduce botrocetin-induced platelet aggregation (*31*). This is the first report describing the identification of cysteine-constrained cyclic peptides, identified by phage display, that bind to human GPIbα and act as potent antiplatelet aggregation agents.

Phage display efforts utilized multiple cysteine-constrained peptide libraries screened against the GPIbα target. The primary selection identified several 9 amino acid disulfide-constrained peptides specific to GPIbα. An optimized library was prepared on the basis of the primary selection consensus sequence and screened against GPIbα to identify key residues important for binding to the target and/or required for proper presentation of the peptide. Second, the optimized library offers a significant opportunity to improve binding affinity by sampling the amino acid sequences of peptides that may not have been present in the primary screen due to incomplete representation in peptide libraries of this length. However, in this case, the optimized selection identified additional peptides specific to the target with their amino acid sequences nearly identical to the primary screen consensus with the exception of the residues at position 4 (Table 2).

The biophysical properties of one primary selection and two optimized selection synthetic peptides were determined by SPR. This analysis allows the accurate determination of K_D values with pure component reagents and confirms that binding is due solely to the identified peptide verses the phage scaffold. Although there was a marginal improvement in the GPIbα binding affinity of OS-2 when compared to the parent peptide PS-4, this analysis revealed nearly a 90-fold K_D value enhancement for the optimized peptide OS-1

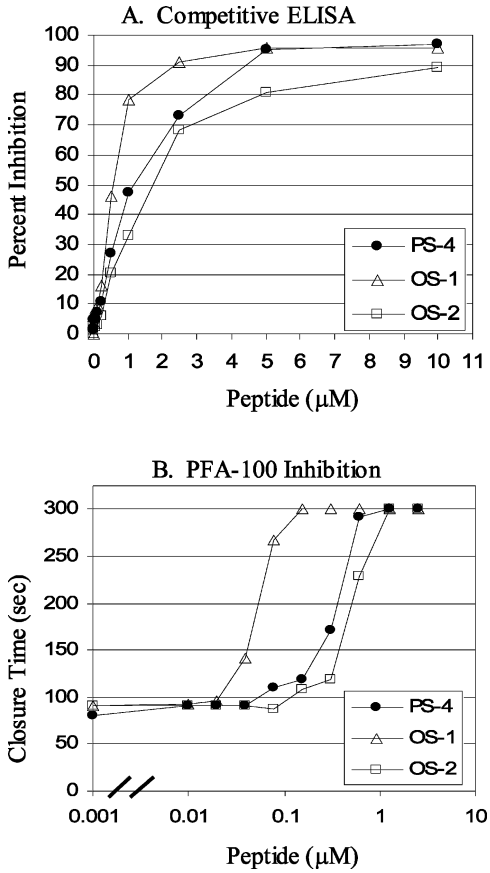

FIGURE 4: (A) Competitive ELISA of the GPIbα-Fc and vWF-A1 domain. The parent PS-4 (●) and optimized OS-1 (△) and OS-2 (□) peptides were tested in an ELISA of GPIbα-Fc binding to immobilized vWF-A1 at a concentration range of 0.002–10 μM. All three peptides inhibited binding in a concentration-dependent manner with calculated IC_{50} values of 1.26, 0.51, and 1.40 μM, respectively. (B) Peptide inhibition of platelet aggregation assessed by PFA-100. High shear-dependent platelet aggregation was inhibited by parent peptide PS-4 (●) and optimized peptides OS-1 (△) and OS-2 (□). OS-1 inhibited platelet aggregation in a concentration-dependent manner, approximately 8-fold more potently than the parent peptide PS-4, with complete inhibition observed at 150 nM.

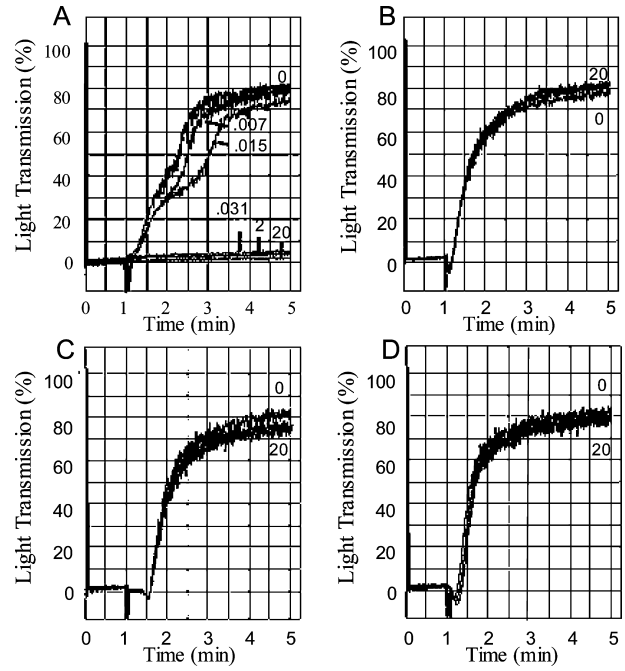

FIGURE 5: Platelet aggregation selectivity of GPIbα binding peptide OS-1. Platelet aggregation was analyzed in an optical aggregometer with agonists acting through the GPIbα pathway (ristocetin) or independent of GPIbα (ADP, collagen, thrombin). Ristocetin-induced platelet agglutination (vWF- and GPIbα-dependent) was completely inhibited by concentrations of OS-1 peptide as low as 31 nM (panel A). In contrast, other agonists were able to induce platelet aggregation (ADP, panel B; collagen, panel C; and γ-thrombin, panel D) and were not blocked in the presence of up to 20 μM OS-1.

verses PS-4. The single amino acid substitution of M for W at position 4 in OS-1 had a positive influence on binding affinity, suggesting that a smaller more flexible hydrophobic amino acid without a bulky aromatic side chain is preferred sterically or alternatively promotes a thermodynamically stable conformation of the peptide. This is further supported by the observation of amino acid diversity at this position in both primary and optimized selections, indicating that the improved binding is not due to a direct single residue interaction with GPIbα. The SPR and ITC determination of PS-4 K_D values were in agreement, and the analysis of binding interaction stoichiometry by ITC supports site-specific GPIbα binding.

NMR line width is an exquisitely sensitive parameter to probe binding. In the context of protein–ligand binding slow exchange that usually accompanies tight binding is characterized by a dramatic increase in the rotational correlation time of the ligand. An increase in correlation time is manifested as a stoichiometric decrease in peak intensity since the transverse relaxation times of the protons in the complex are too short to be detected. However, in the intermediate exchange regime, the line width is dominated by the chemical exchange mechanism. In this regime, the relative population of the free and bound forms governs both the peak position and the line width, in addition to the rate of exchange between the two forms. The change in line width is also dictated by the relaxation rates in the free and bound forms. As seen in Figure 3, addition of GPIbα to vWF-A1 results in line broadening indicating an exchange between free vWF-A1 and vWF-A1 bound to GPIbα. The addition of OS-1 to a mixture of GPIbα and vWF-A1 partially reverses this line broadening, suggesting that OS-1 and vWF-A1 share a common binding site on GPIbα.

ITC was used to further characterize the PS-4 binding site on GPIbα. The K_D of PS-4 was determined with GPIbα protein having the amino acid substitutions G233V and/or M239V to evaluate the effect these mutations have on peptide binding. These genetic mutations were originally reported in patients with platelet-type von Willebrand disease (VWD) (*32–34*). Platelet-type VWD is a subset of the more common forms of VWD. Substitutions associated with this phenotype have been identified within the vWF-A1 binding region on GPIbα and include amino acids G233 and M239. These mutations induce shear-independent binding of GPIbα to vWF, resulting in a reduction of circulating high molecular weight vWF multimers and subsequent thrombocytopenia (*35*). The X-ray crystal structure of the GPIbα−vWF-A1 complex revealed two key and extensive binding interfaces on the concave face of GPIbα. One of these, the C-terminal β-switch region, includes the amino acids from G233 to M239. Subtle differences in the structure of the GPIbα-flexible β-switch region are predicted to stabilize and initiate

or prime the association with vWF-A1 (*13, 14*). Interestingly, the K_D value determined using ITC between PS-4 and GPIbα M239V (data not shown) was 2.2 μM, a binding affinity more than 30-fold weaker when compared to the same peptide and wild-type GPIbα. In addition, ITC analysis was unable to detect binding between PS-4 and the GPIbα protein possessing both the M239V and G233V GPIbα β-switch region substitutions (data not shown). These corroborating data suggest that peptide PS-4 may in fact bind directly to the β-switch region of GPIbα. However, confirmation and precise mapping of the PS-4 binding site location on GPIbα requires further investigation.

A flow cytometry platelet aggregation assay and biochemical ELISA were performed to initiate the characterization of PS-4, OS-1, and OS-2 inhibitory properties (Figure 4). This assay used a platelet function analyzer (PFA-100) to flow a peptide titration series with human whole blood, through an agonist-coated capillary simulating in vivo high shear stress conditions and primary hemostasis (*36*). The aggregation of platelets and cessation of blood flow at each concentration of peptide through the capillary provide end point closure times necessary for the determination of IC_{50} values. All three peptides evaluated with the PFA-100 under these simulated physiological conditions were able to inhibit platelet aggregation, and the results showed that OS-1 was the most potent inhibitor of aggregation. The ranking of inhibition for peptides PS-4, OS-1, and OS-2 determined by the platelet aggregation assay was consistent with the IC_{50} values obtained using a competitive ELISA and purified protein components. These results also correlated well with the SPR kinetic analysis that showed the most efficacious peptide inhibitor OS-1 had the fastest association rate and slowest dissociation rate (data not shown). Conversely, the fast dissociation rate exhibited by peptide OS-2 may explain its less potent inhibitory effect. Combining the flow cytometry, ELISA, and SPR analysis confirmed that the selected peptides inhibited hemostasis under simulated physiological conditions and identified peptide inhibition specific to the vWF-A1 and GPIbα interaction.

To demonstrate relevant physiological specificity of OS-1 for the GPIbα signaling pathway, the platelet aggregation capability of OS-1 was measured using optical aggregation. This assay combined platelet-rich plasma, peptide OS-1, a platelet aggregation agonist, and generated a real time measurement of optical aggregation. This blockade clearly occurred with ristocetin, a modulator that acts on vWF in a manner dependent upon the GPIbα pathway. However, when aggregation was induced by the agonists ADP, collagen, and thrombin, which operate independent of GPIbα signaling, OS-1 did not block platelet aggregation. These data clearly indicate peptide OS-1 as an inhibitor of platelet aggregation via the GPIbα signaling pathway.

Since one of the earliest events leading to platelet aggregation under high shear occurs between GPIbα and vWF bound to the subendothelial collagen matrix of damaged vasculature, disrupting platelet aggregation by targeting platelet GPIbα interactions with vWF offers a powerful approach to reducing platelet-driven thrombus formation and represents an attractive pharmaceutical target (reviewed in refs *37–41*. Identifying potent inhibitors of high shear-dependent platelet aggregation would ideally target events crucial for pathological thrombus formation with minimal impact on normal hemostasis. The information gained from the analysis of GPIbα with inhibitory peptides, and further investigation to acquire costructures, may ultimately prove useful for the development of small-molecule GPIbα−vWF-A1 antagonists and provide new therapies for the treatment of thrombotic diseases.

ACKNOWLEDGMENT

We gratefully acknowledge Erik Feyfant for help with modeling and Lidia Mosyak for critical review of the manuscript, Ravindra Kumar and Ella Presman for expression of GPIbα, Karl Malakian and Scott Wolfrom for expression of vWF, and the DNA sequencing group led by Jan Kieleczawa.

REFERENCES

1. Ruggeri, Z. M. (2004) Platelet and von Willebrand factor interactions at the vessel wall. *Haemostaseologie 24*, 1–11.
2. Andrews, R. K., Gardiner, E. E., Shen, Y., Whisstock, J. C., and Berndt, M. C. (2003) Glycoprotein Ib-IX-V. *Int. J. Biochem. Cell Biol. 35*, 1170–1174.
3. Berndt, M. C., Shen, Y., Dopheide, S. M., Gardiner, E. E., and Andrews, R. K. (2001) The vascular biology of the glycoprotein Ib-IX-V complex. *Thromb. Haemostasis 86*, 178–188.
4. Fujimura, Y., Titani, K., Holland, L. Z., Russell, S. R., Roberts, J. R., Elder, J. H., Ruggeri, Z. M., and Zimmerman, T. S. (1986) von Willebrand factor. A reduced and alkylated 52/48-kDa fragment beginning at amino acid residue 449 contains the domain interacting with platelet glycoprotein Ib. *J. Biol. Chem. 261*, 381–385.
5. Siedlecki, C. A., Lestini, B. J., Kottke-Marchant, K. K., Eppell, S. J., Wilson, D. L., and Marchant, R. E. (1996) Shear-dependent changes in the three-dimensional structure of human von Willebrand factor. *Blood 88*, 2939–2950.
6. Marshall, S. J., Senis, Y. A., Auger, J. M., Feil, R., Hofmann, F., Salmon, G., Peterson, J. T., Burslem, F., and Watson, S. P. (2004) GPIb-dependent platelet activation is dependent on Src kinases but not MAP kinase or cGMP-dependent kinase. *Blood 103*, 2601–2609.
7. Kasirer-Friede, A., Cozzi, M. R., Mazzucato, M., De Marco, L., Ruggeri, Z. M., and Shattil, S. J. (2004) Signaling through GP Ib-IX-V activates alpha IIb beta 3 independently of other receptors. *Blood 103*, 3403–3411.
8. Ozaki, Y., Asazuma, N., Suzuki-Inoue, K., and Berndt, M. C. (2005) Platelet GPIb-IX-V-dependent signaling. *J. Thromb. Haemostasis 3*, 1745–1751.
9. Uff, S., Clemetson, J. M., Harrison, T., Clemetson, K. J., and Emsley, J. (2002) Crystal structure of the platelet glycoprotein Ib(alpha) N-terminal domain reveals an unmasking mechanism for receptor activation. *J. Biol. Chem. 277*, 35657–35663.
10. Emsley, J., Cruz, M., Handin, R., and Liddington, R. (1998) Crystal structure of the von Willebrand Factor A1 domain and implications for the binding of platelet glycoprotein Ib. *J. Biol. Chem. 273*, 10396–10401.
11. Handa, M., Titani, K., Holland, L. Z., Roberts, J. R., and Ruggeri, Z. M. (1986) The von Willebrand factor-binding domain of platelet membrane glycoprotein Ib. Characterization by monoclonal antibodies and partial amino acid sequence analysis of proteolytic fragments. *J. Biol. Chem. 261*, 12579–12585.
12. Vicente, V., Kostel, P. J., and Ruggeri, Z. M. (1988) Isolation and functional characterization of the von Willebrand factor-binding domain located between residues His1-Arg293 of the alpha-chain of glycoprotein Ib. *J. Biol. Chem. 263*, 18473–18479.
13. Huizinga, E. G., Tsuji, S., Romijn, R. A., Schiphorst, M. E., de Groot, P. G., Sixma, J. J., and Gros, P. (2002) Structures of glycoprotein Ibalpha and its complex with von Willebrand factor A1 domain. *Science 297*, 1176–1179.
14. Dumas, J. J., Kumar, R., McDonagh, T., Sullivan, F., Stahl, M. L., Somers, W. S., and Mosyak, L. (2004) Crystal structure of the wild-type von Willebrand factor A1-glycoprotein Ibalpha complex reveals conformation differences with a complex bearing von Willebrand disease mutations. *J. Biol. Chem. 279*, 23327–23334.
15. Cochran, A. J. (2000) *Chem. Biol. 9*, R85–R94.

16. Cwirla, S. E., Peters, E. A., Barrett, R. W., and Dower, W. J. (1990) Peptides on phage: a vast library of peptides for identifying ligands. *Proc. Natl. Acad. Sci. U.S.A. 87*, 6378–6382.
17. Thanos, C. D., Randal, M., and Wells, J. A. (2003) Potent small-molecule binding to a dynamic hot spot on IL-2. *J. Am. Chem. Soc. 125*, 15280–15281.
18. Arkin, M. R., and Wells, J. A. (2004) Small-molecule inhibitors of protein-protein interactions: progressing towards the dream. *Nat. Rev. Drug Discov. 3*, 301–317.
19. DeLano, W. L., Ultsch, M. H., de Vos, A. M., and Wells, J. A. (2000) Convergent solutions to binding at a protein-protein interface. *Science 287*, 1279–1283.
20. Kenny, C. H., Ding, W., Kelleher, K., Benard, S., Dushin, E. G., Sutherland, A. G., Mosyak, L., Kriz, R., and Ellestad, G. (2003) Development of a fluorescence polarization assay to screen for inhibitors of the FtsZ/ZipA interaction. *Anal. Biochem. 323*, 224–233.
21. McDowell, R. S., Blackburn, B. K., Gadek, T. R., McGee, L. R., Rawson, T., Reynolds, M. E., Robarge, K. D., Somers, T. C., Thorsett, E. D., Tischler, M., Webb, R. R., II, and Venuti, M. C. (1994) From peptide to non-peptide. 2. The de novo design of potent, non-peptidal inhibitors of platelet aggregation based on a benzodiazepinedione scaffold. *J. Am. Chem. Soc. 116*, 5077–5083.
22. McDowell, R. S., Elias, K. A., Stanley, M. S., Burdick, D. J., Burnier, J. P., Chan, K. S., Fairbrother, W. J., Hammonds, R. G., Ingle, G. S., Jacobsen, N. E., Mortensen, D. L., Rawson, T. E., Won, W. B., Clark, R. G., and Somers, T. C. (1995) Growth hormone secretagogues: characterization, efficacy, and minimal bioactive conformation. *Proc. Natl. Acad. Sci. U.S.A. 92*, 11165–11169.
23. Geysen, H. M., Rodda, S. J., Mason, T. J., Tribbick, G., and Schoofs, P. G. (1987) Strategies for epitope analysis using peptide synthesis. *J. Immunol. Methods 102*, 259–274.
24. Tesmer, J. J. (2006) Pharmacology. Hitting the hot spots of cell signaling cascades. *Science 312*, 377–378.
25. James, G. L., Goldstein, J. L., Brown, M. S., Rawson, T. E., Somers, T. C., McDowell, R. S., Crowley, C. W., Lucas, B. K., Levinson, A. D., and Marsters, J. C., Jr. (1993) Benzodiazepine peptidomimetics: potent inhibitors of Ras farnesylation in animal cells. *Science 260*, 1937–1942.
26. Wrighton, N. C., Farrell, F. X., Chang, R., Kashyap, A. K., Barbone, F. P., Mulcahy, L. S., Johnson, D. L., Barrett, R. W., Jolliffe, L. K., and Dower, W. J. (1996) Small peptides as potent mimetics of the protein hormone erythropoietin. *Science 273*, 458–464.
27. Fairbrother, W. J., Christinger, H. W., Cochran, A. G., Fuh, G., Keenan, C. J., Quan, C., Shriver, S. K., Tom, J. Y., Wells, J. A., and Cunningham, B. C. (1998) Novel peptides selected to bind vascular endothelial growth factor target the receptor-binding site. *Biochemistry 37*, 17754–17764.
28. Kageyama, S., Yamamoto, H., Nakazawa, H., Matsushita, J., Kouyama, T., Gonsho, A., Ikeda, Y., and Yoshimoto, R. (2002) Pharmacokinetics and pharmacodynamics of AJW200, a humanized monoclonal antibody to von Willebrand factor, in monkeys. *Arterioscler. Thromb. Vasc. Biol. 22*, 187–192.
29. Hennan, J., Swillo, R., Morgan, G., Leik, C., Brooks, J., Shaw, G., Schaub, R., Crandall, D., and Vlasuk, G. (2006) Pharmacologic inhibition of platelet vWF-GP1-alpha interaction prevents coronary artery thrombosis. *Thromb. Haemostasis 95*, 469–475.
30. Wadanoli, M., Sako, D., Shaw, G. D., Schaub, R. G., Wang, Q., Tchernychev, B., Xu, J., Porter, T. J., and Huang, Q. (2007) The von Willebrand factor antagonist (GPG-290) prevents coronary thrombosis without prolongation of bleeding time. *Thromb. Haemostasis 98*, 397–405.
31. McGhie, A. I., McNatt, J., Ezov, N., Cui, K., Mower, L. K., Hagay, Y., Buja, L. M., Garfinkel, L. I., Gorecki, M., and Willerson, J. T. (1994) Abolition of cyclic flow variations in stenosed, endothelium-injured coronary arteries in nonhuman primates with a peptide fragment (VCL) derived from human plasma von Willebrand factor-glycoprotein Ib binding domain. *Circulation 90*, 2976–2981.
32. Miller, J. L., Cunningham, D., Lyle, V. A., and Finch, C. N. (1991) Mutation in the gene encoding the alpha chain of platelet glycoprotein Ib in platelet-type von Willebrand disease. *Proc. Natl. Acad. Sci. U.S.A. 88*, 4761–4765.
33. Takahashi, H., Murata, M., Moriki, T., Anbo, H., Furukawa, T., Nikkuni, K., Shibata, A., Handa, M., Kawai, Y., and Watanabe, K. (1995) Substitution of Val for Met at residue 239 of platelet glycoprotein Ib alpha in Japanese patients with platelet-type von Willebrand disease. *Blood 85*, 727–733.
34. Wang, Q., Shorten, D., Xu, X., Shaw, G. D., Schaub, R. G., Shea, C., Brooks, J., Sako, D., Wiswall, E., Xu, J., Szklut, P., and Patel, V. S. (2006) Effect of von Willebrand factor on the pharmacokinetics of recombinant human platelet glycoprotein Ibalpha-immunoglobulin G1 chimeric proteins. *Pharm. Res. 23*, 1743–1749.
35. Doggett, T. A., Girdhar, G., Lawshe, A., Miller, J. L., Laurenzi, I. J., Diamond, S. L., and Diacovo, T. G. (2003) Alterations in the intrinsic properties of the GPIbalpha-VWF tether bond define the kinetics of the platelet-type von Willebrand disease mutation, Gly233Val. *Blood 102*, 152–160.
36. Favaloro, E. J., Facey, D., and Henniker, A. (1999) Use of a novel platelet function analyzer (PFA-100) with high sensitivity to disturbances in von Willebrand factor to screen for von Willebrand's disease and other disorders. *Am. J. Hematol. 62*, 165–174.
37. Vanhoorelbeke, K., Ulrichts, H., Schoolmeester, A., and Deckmyn, H. (2003) Inhibition of platelet adhesion to collagen as a new target for antithrombotic drugs. *Curr. Drug Targets Cardiovasc. Haematol. Disord. 3*, 125–140.
38. Gresele, P., and Agnelli, G. (2002) Novel approaches to the treatment of thrombosis. *Trends Pharmacol. Sci. 23*, 25–32.
39. Labuzek, K., Krysiak, R., Okopien, B., and Herman, Z. S. (2003) Progress in pharmacotherapy of thrombosis. *Pol. J. Pharmacol. 55*, 523–533.
40. Jackson, S. P., and Schoenwaelder, S. M. (2003) Antiplatelet therapy: in search of the "magic bullet". *Nat. Rev. Drug Discov. 2*, 775–789.
41. Bonnefoy, A., Vermylen, J., and Hoylaerts, M. F. (2003) Inhibition of von Willebrand factor-GPIb/IX/V interactions as a strategy to prevent arterial thrombosis. *Expert Rev. Cardiovasc. Ther. 1*, 257–269.

BI702428Q